


Safety of Intraovarian Injection of Human Mesenchymal Stem Cells in a Premature Ovarian Insufficiency Mouse Model

Cell Transplantation
Volume 30: 1–13
© The Author(s) 2021
Article reuse guidelines:
sagepub.com/journals-permissions
DOI: 10.1177/0963689720988502
journals.sagepub.com/home/cll


Hang-Soo Park^{1,*} , Rishi Man Chugh^{2,*}, Amro Elsharoud²,
Mara Ulin², Sahar Esfandiyari², Alshimaa Aboalsoud^{2,3},
Lale Bakir², and Ayman Al-Hendy¹

Abstract

Primary ovarian insufficiency (POI), a condition in which there is a loss of ovarian function before the age of 40 years, leads to amenorrhea and infertility. In our previously published studies, we demonstrated recovery of POI, correction of serum sex hormone levels, increase in the granulosa cell population, and restoration of fertility in a chemotherapy-induced POI mouse model after intraovarian transplantation of human bone marrow-derived mesenchymal stem cells (hBM-MSCs). While hBM-MSC may be a promising cell source for treatment of POI, there are few reports on the safety of stem cell-based therapy for POI. For future clinical applications, the safety of allogenic hBM-MSCs for the treatment of POI through intraovarian engraftment needs to be addressed and verified in appropriate preclinical models. In this study, we induced POI in C57/BL6 mice using chemotherapy, then treated the mice with hBM-MSCs (500,000 cells/ovary) by intraovarian injection. After hBM-MSC treatment, we analyzed the migration of engrafted cells by genomic DNA polymerase chain reaction (PCR) using a human-specific ALU repeat and by whole-body sectioning on a cryo-imaging system. We examined the possibility of transfer of human DNA from the hBM-MSCs to the resulting offspring, and compared the growth rate of offspring to that of normal mice and hBM-MSC-treated mice. We found that engrafted hBM-MSCs were detected only in mouse ovaries and did not migrate into any other major organs including the heart, lungs, and liver. Further, we found that no human DNA was transferred into the fetus. Interestingly, the engrafted cells gradually decreased in number and had mostly disappeared after 4 weeks. Our study demonstrates that intraovarian transplantation of hBM-MSCs could be a safe stem cell-based therapy to restore fertility in POI patients.

Keywords

mesenchymal stem cell, primary ovarian insufficiency, toxicology

Introduction

Primary ovarian insufficiency (POI), also known as premature ovarian failure, is defined as an early loss of ovarian function before the age of 40 years, which usually manifests as amenorrhea and infertility^{1–3}. The annual incidence of POI has been steadily increasing^{4,5}. Approximately 70% of POI cases are idiopathic, and while evaluation is warranted to identify the underlying etiology⁶, in many cases it is not clear. Iatrogenic POI secondary to chemotherapy is frequently reported and its incidence has been increasing, accounting for approximately half of the new cases of POI in women (20% to 80%) of reproductive age^{7,8}. Chemotherapy inhibits the growth of tumor cells; however, it also causes apoptosis of granulosa cells, follicular atresia, and

decreased ovarian function, which leads to the clinical manifestations of POI^{9–11}.

¹ Department of Obstetrics and Gynecology, University of Chicago, IL, USA

² Department of Surgery, College of Medicine, University of Illinois at Chicago, IL, USA

³ Faculty of Medicine, Department of Pharmacology, Tanta University, Egypt

* Both the authors contributed equally to this article

Submitted: July 30, 2020. Revised: November 20, 2020. Accepted: December 29, 2020.

Corresponding Author:

Ayman Al-Hendy, Department of Obstetrics and Gynecology, University of Chicago, 5841 S. Maryland Ave, Chicago, IL 60637, USA.
Email: aalhendy@BSD.Uchicago.edu



As there are no treatments that restore ovarian function in women with POI, the only option to achieve pregnancy is egg donation from a healthy donor. Recently, researchers have evaluated cell-based therapy using mesenchymal stem cells (MSCs) as a treatment option for POI-associated infertility^{10,12–14}. A recent study reported that MSCs repair injured cells via paracrine activity or direct cell-to-cell interaction¹⁵. In a previous study, we reported that transplantation of MSCs in a chemotherapy-induced POI mouse ovary corrected serum hormonal levels, restored the granulosa cell population, and stimulated ovarian follicle and angiogenesis, leading to a higher successful pregnancy rate compared to untreated POI mice^{16–18}.

Though the therapeutic potential of MSCs in various disease conditions is well documented, safety concerns in using allogenic MSC as a biological drug remain. Several recent studies have raised concerns about potential side effects of exogenous stem cells after transplantation, such as tumor formation and neoplastic transformation^{19,20}. Although MSCs have proven to be a safer source of stem cells compared to other types of pluripotent stem cells^{21,22}, they carry an inherent risk of tumor-like mass formation^{23,24}.

To realize the translational potential and clinical application of MSCs in the treatment of POI-associated infertility, we evaluated the safety and the potential risk of allogenic MSC treatment in a well-established preclinical mouse model of chemotherapy-induced POI^{25,26}. These mice show a reduced number of ovarian follicles and abnormal serum hormones level after 7 days of treatment with cyclophosphamide and busulphan. After transplantation of human bone marrow MSCs (hBM-MSCs) by direct intraovarian injection, as established in our previous study¹⁷, we traced the migration of engrafted cells and examined the possibility of transfer of human DNA from the hBM-MSCs to offspring.

Materials and Methods

hBM-MSC Cell Culture

hBM-MSCs were purchased from Roosterbio (Frederick, MD, USA); these cells were isolated from the bone marrow of a 29-year-old female and 26-year-old female. hBM-MSCs were cultured in the recommended cell culture medium, RoosterNourish-MSC-XF (Roosterbio, Frederick, MD, USA). At approximately 80% confluence, the cells were trypsinized using CTS TrypLE select enzyme (Gibco, Waltham, MA, USA) and serially expanded for two additional passages. At the end of the culture expansion, hBM-MSCs were collected and centrifuged at $200 \times g$ for 8 min. For intraovarian injection, 5×10^5 hBM-MSCs were resuspended with $10 \mu\text{l}$ phosphate-buffered saline (PBS).

Fluorescence Labeling and Microscopy

For hBM-MSC fluorescence labeling, hBM-MSCs were incubated in the culture medium containing Molday ION Rhodamine B (MIRB) at a final concentration of $30 \mu\text{g/ml}$

of medium. After 20 h of incubation, medium containing MIRB was replaced with fresh culture medium after washing with PBS. Fluorescence was observed using an EVOS FL fluorescence microscope (Thermo Fisher Scientific, Waltham, MA, USA).

POI Mouse Model

The experimental animal protocol in this study was approved by the University of Illinois at Chicago Animal Care Committee, and all animal experiments were performed in accordance with the ethical policy and guidelines of University of Illinois at Chicago for laboratory animals. We used the chemotherapy-induced POI animal model and hBM-MSC intraovarian injection protocol as established and described in our previous study^{16,17}. Briefly, female C57BL6 mice were treated with busulphan (30 mg/kg) and cyclophosphamide (120 mg/kg) by intraperitoneal injection. The control group was treated with PBS. After 7 days of chemotherapy, hBM-MSCs were transplanted into the ovary by intraovarian injection, as follows. All mice were treated preoperatively with one dose of buprenorphine (0.1 mg/kg) and anesthetized using 1% to 4% isoflurane inhalation. A small incision on the skin was made to access the ovary via the caudal abdominal cavity, and the uterine horns were traced to identify the ovary. Then, 5×10^5 hBM-MSCs resuspended in $10 \mu\text{l}$ PBS were injected into each ovary. For the control and untreated POI groups, $10 \mu\text{l}$ PBS was injected into each ovary. Seven days after hBM-MSC treatment, two female mice were housed with one C57BL6 male mouse for breeding. Pregnancy rate per group was calculated as “number of pregnant mouse/number of all mouse in group.” After delivery, the postnatal pup body weight was measured at day 0, day 5, and day 10.

Estrous Cycle Monitoring

Estrous cycles were monitored daily for 14 days after initiation of chemotherapy to verify chemotherapy-induced POI. Daily vaginal swab samples were performed using clean and sterile cotton swabs and smeared onto a clean glass slide for staining and evaluation of estrous cycle stage. Each slide was stained with 0.1% crystal violet solution for 1 min following a published protocol²⁷. The estrous cycle stage was examined by bright field microscopy based on the presence or absence of nucleated epithelial cells and leukocytes^{27,28}.

Histology

Ovarian tissue was collected 2 weeks after hBM-MSC transplantation for histological analysis. Ovaries were fixed immediately with 10% neutral buffered formalin, then processed for paraffin embedding, sectioning, and staining for hematoxylin and eosin (H&E) and immunohistochemistry (IHC) in the UIC Research Histology and Tissue Imaging Core. CD31 (Cell Signaling, Danvers, MA, USA, 77699 S, 1:200), estrogen receptor (ER α) (Thermo Fisher, Waltham, MA, 5-14501,

1:20,000), progesterone receptor (PR; Biocompare, South San Francisco, CA, USA, ACA 302 A, 1:200), and Ki67 antibodies (Abcam, Cambridge, MA, USA, ab16667, 1:200) were used for IHC. For TUNEL assay, TUNEL Assay Kit-HRO-DAB (Abcam, ab206386) was used. For quantification of IHC, whole stained slides were scanned using a Leica Aperio AT2 camera (Leica, Wetzlar, Germany) and analyzed using Aperio ImageScope software (v12.4.0.5043). In each image, the ovarian tissue area was selected manually and positivity (positive area/total area) was analyzed in the selected area by an internal algorithm, Positive Pixel Count V9.

Reverse Transcriptase Polymerase Chain Reaction (RT-PCR)

RNA isolation was performed using TRIzol Reagent (Invitrogen, Waltham, MA, USA) according to the manufacturer's instructions. RNA concentration was quantified by spectrophotometry at 260 nm using Nanodrop 2000 (Thermo Fisher Scientific). A total of 1 µg of RNA was reverse transcribed to prepare cDNA using the RNA to cDNA EcoDry premix (Takara Bio, Kusatsu, Shiga, Japan). Real-time PCR was performed using the CFX96 PCR instrument with matched primers (Table 1) and Universal SYBR Green Supermix (Bio-Rad, Hercules, CA, USA). The following PCR parameters were used: initial denaturation cycle at 95°C for 3 min, followed by 40 amplification cycles at 95°C for 10 s, 56°C for 15 s, and 72°C for 1 min. The results are presented as the fold change in relative gene expression quantified using the delta-delta CT method.

Human Cell Detection by Genomic DNA PCR

For genomic DNA isolation, 25 to 50 mg of mouse tissue was mechanically homogenized with 1 ml DNazol reagent (Thermo Fisher Scientific). Homogenate was centrifuged at 10,000 × g for 10 min at room temperature, and the supernatant was transferred into a fresh tube. For DNA precipitation, 0.5 ml of 100% ethanol was added into the supernatant. Genomic DNA was isolated following the manufacturer's protocol. The concentration of DNA was quantified using Nanodrop 2000 (Thermo Fisher Scientific).

For human cell detection by PCR, a human-specific ALU primer sequence was used as described in the literature²⁹. Genomic DNA PCR was performed with ALU primers under the following conditions: one cycle of 95° for 10 min, followed by 50 cycles of 95° for 15 s, 56° for 30 s, and 72° for 30 s. The number of human cells in each sample was calculated using the correlation between CT value and cell number in the positive control sample.

Fluorescence Cryo-Imaging

To detect MIRB-labeled hBM-MSCs in mice, whole-animal cryo-imaging was performed on a CryoViz Instrument (BioInvision, Cleveland, OH, USA). Mice were treated with

Table 1. Primer Sequences for Polymerase Chain Reaction.

Gene	Sequence (5'-3')
Mouse GAPDH F	CACATTGGGGGTAGGAACAC
Mouse GAPDH R	AACTTTGGCATTGTGGAAGG
Mouse FSHR F	GTGCATTCAACGGAACCCAG
Mouse FSHR R	TCTAAGCCATGGTTGGGCAG
Mouse CYP19a1 F	TTTCGCTGAGAGACGTGGAG
Mouse CYP19a1 R	AGGATTGCTGCTTCGACCTC
Mouse ERα F	AATTCTGACAATCGACGCCAG
Mouse ERα R	GTGCTTCAACATTCTCCCTCCTC
Mouse PR F	GGTGGAGGTCGTACAAGCAT
Mouse PR R	GGATTTGCCACATGGTAAGG
Mouse Ki67 F	CTGCCTGCGAAGAGAGCATC
Mouse Ki67 R	AGCTCCACTTCGCCTTTTGG
Mouse TGFβ F	ATACGTCAGACATTCCGGAAGCAGTG
Mouse TGFβ R	AATAGTTGGTATCCAGGGCTCTCCG
Mouse Bcl2 F	GTGGTGGAGGAACCTCTCA
Mouse Bcl2 R	GTTCCACAAAGGCATCCCAG
Mouse VEGFA F	GTACCTCCACCATGCCAAAGT
Mouse VEGFA R	GCATTTCACATCTGTGTGCT
Mouse αSMA F	GGCTCTGGGCTCTGTAAGG
Mouse αSMA R	CTCTTGCTCTGGGCTTCATC
Human ALU F	GGTGAAACCCCGTCTCTACT
Human ALU R	GGTTCAAGCGATTCTCCTGC

MIRB-labeled hBM-MSCs by intraovarian injection. Mice were euthanized, embedded in cyro-imaging embedding compound (BioInvision), and immediately frozen in liquid nitrogen. The frozen blocks were sent to the BioInvision Cryo-imaging lab (Mayfield Village, OH, USA) for imaging and analysis using their CryoViz Instrument.

Statistical Analysis

mRNA and protein levels of the examined markers were treated as continuous variables and expressed as means ± standard deviations. Analysis of variance and Bonferroni's multiple-comparisons post hoc testing were used to compare the groups. The significance level was set at 5% ($P < 0.05$). The SPSS statistical program (version 22) was used to analyze the data.

Results

Intraovarian Engraftment of hBM-MSCs Restores Fertility in a POI Mouse Model

We induced POI in mice by injecting chemotherapeutic agents (120 mg/kg of cyclophosphamide and 30 mg/kg of busulfan) via intraperitoneal injection. Estrus cycle stage was analyzed to confirm the POI induction. Through bright field microscopy of vaginal smear sample, each estrus cycle was identified (Fig. 1A). Proestrus (Fig. 1A upper-left) was presented by nucleated epithelial cells (red arrow) without leukocyte. Estrus (Fig. 1A upper-right) was identified by cornified epithelial cells (white arrow) without leukocyte. Metestrus (lower-left) showed both cornified epithelial cells

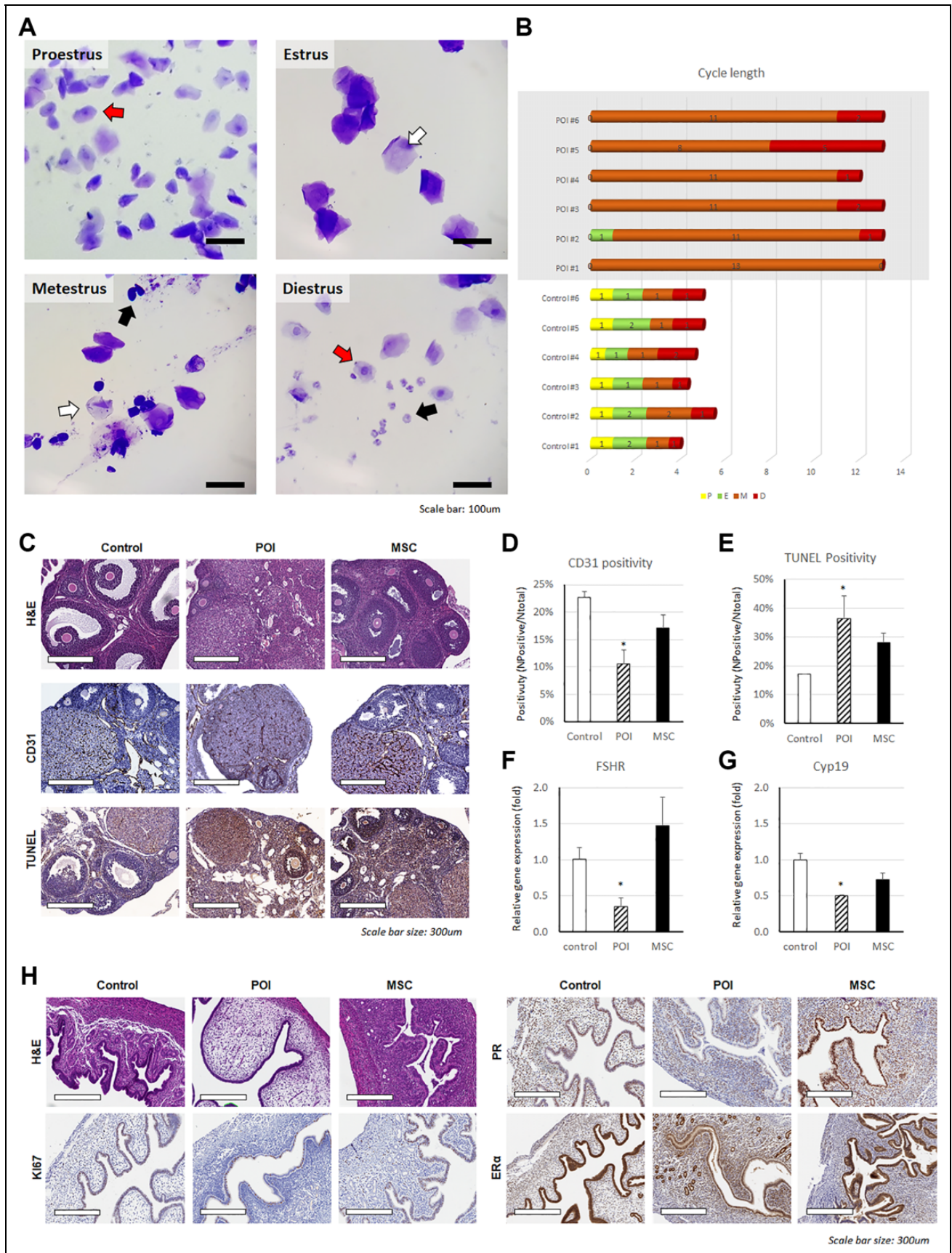


Figure 1. Generation of the chemotherapy-induced POI mouse model and reversal of POI characteristics after intraovarian injection of hBM-MSC. (A) Representative image of the mouse vaginal swab sampling in each estrous cycle (scale bar size: 100 μm). (B) Average cycle length (to be Continued.)

(white arrow) and leukocyte (black arrow) while diestrus (lower-right) showed nucleated epithelial cells (red arrow) with leukocyte (black arrow). As expected^{25,26}, 7 days after chemotherapy, mice showed an altered estrous cycle arrested in metestrus and diestrus, whereas normal mice maintained normal 4- to 5-day estrous cycle (Fig. 1A, B). After inducing POI, we transplanted hBM-MSCs (500,000 cells/10 μ l) in each ovary. Consistent with our previous study¹⁷, intraovarian injection of hBM-MSCs reversed abnormal ovarian morphology in the POI mice (Fig. 1C-H), including the restoration of follicle numbers. Furthermore, we analyzed vascularization of the ovary tissue using the vascular endothelial cell marker CD31 by IHC and ovarian cell apoptosis by TUNEL assay (Fig. 1C-E). The extent of CD31-positive ovarian microvasculature was decreased in the POI mouse model (10.56% \pm 2.58%) and significantly recovered by hBM-MSC treatment (17.06% \pm 2.46%). The number of TUNEL-positive ovarian cells was significantly higher in POI mice (36.50% \pm 7.77%, $P < 0.05$) and showed a trend toward decreased apoptosis after hBM-MSC treatment (28.11% \pm 3.18%). The average intensity of TUNEL-positive cells was also high in the POI ovary (4.00 \pm 1.66-fold) and decreased after hBM-MSC treatment (2.03 \pm 0.97-fold).

We also analyzed the mRNA expression level of several steroidogenesis-related genes in ovary tissue (Fig. 1F, G). Expression of the ovarian granulosa cell marker FSHR was significantly decreased in the POI mouse ovary (0.35 \pm 0.12-fold) and this loss was reversed after hBM-MSC engraftment (1.47 \pm 0.39-fold, $P < 0.05$). The estrogen synthesis marker CYP19A1 (Cyp19) gene expression was also decreased (0.50 \pm 0.01-fold) in the ovaries of POI mice and restored in the hBM-MSC-engrafted ovary (0.72 \pm 0.09-fold, $P < 0.05$). We also found changes in gene expression in the endometrium of the uterus of POI mice with and without hBM-MSC treatment (Fig. 1H, Supplemental Figure 1A-E). In the POI mouse, endometrial tissue showed reduced expression of ER α (0.23 \pm 0.08-fold), PR (0.12 \pm 0.02-fold), and proliferation marker Ki67 (0.60 \pm 0.09-fold) compared to the normal (control) mouse endometrium. Interestingly, in the hBM-MSC-engrafted POI mouse endometrium, these gene expression changes were reversed for ER α (0.52 \pm 0.06-fold), PR (0.38 \pm 0.03-fold), and Ki67 (1.01 \pm 0.11-fold) compared to control mice. Transforming growth factor β (TGF β) gene expression, which is promoting

preimplantation and angiogenesis, also restored by MSC transplantation (1.63 \pm 0.10-fold). The anti-apoptosis marker BCL2 gene expression, which was decreased in POI (0.44 \pm 0.05-fold), also increased in MSC-treated mouse (2.02 \pm 0.17-fold). Both angiogenesis markers vascular endothelial growth factor A (VEGFA) and α smooth muscle actin were significantly decreased in the POI model, and only VEGFA was significantly restored in the MSC-treated mouse (0.52 \pm 0.16-fold). Taken together, these results confirmed the phenotypic characteristics of POI mice, including estrous cycle arrest, abnormal ovarian morphology and vascularization, and low expression of marker genes in both the ovary and endometrium, and verified that hBM-MSC transplantation was able to reverse these POI-associated changes.

Human Stem Cell Distribution (Detected by PCR) After Intraovarian Injection

To detect engrafted human cells in the mouse body after hBM-MSC injection, we used human-specific ALU-base quantification, as reported in a previously published paper²⁹. We injected PBS (0 cells), 300,000 hBM-MSCs, or 500,000 hBM-MSCs into each mouse ovary. Approximately 5 min after injection, each ovary injected with a different number of hBM-MSCs was collected for genomic DNA isolation. Genomic DNA from the ovary was analyzed by real-time PCR using the human ALU sequence primer. We generated the following equation to calculate the number of human cells in mouse tissue based on the CT value from the PCR analysis (Fig. 2A).

We verified our equation by calculating the CT value of genomic DNA PCR using independent samples; the equation demonstrated 95% to 114% accuracy in quantifying human cells in mouse tissue (Fig. 2B).

To analyze the human cells remaining in our POI mouse model after hBM-MSC transplantation, we collected ovary, uterus, spleen, liver, heart, and lung tissue at 14 and 28 days after transplantation (Fig. 2C, Supplemental Figure 2). On day 14 after transplantation, human cells were detected only in the ovary (approximately 170,000 \pm 96,000 cells). Other tissues such as uterus, spleen, liver, heart, and lung did not contain any human cells. By day 28, only one mouse was found to contain human cells in the ovary (236,000 \pm 3,000 cells); the remaining mice did not contain any human cells in any tissues tested. We repeated the analysis with the hBM-MSCs isolated from

Figure 1. (Continued). length of control and POI mice ($n = 6$ /group). (C) Histological analysis of mouse ovary from a normal mouse (control), POI mouse (POI), and hBM-MSC-treated POI mouse (MSC). H&E staining images for general morphology and folliculogenesis (upper), immunohistochemistry assay using CD31 for angiogenesis (middle), TUNEL assay for ovarian apoptosis (lower) (scale bar size: 300 μ m). (D-E) Quantification of CD31 expression (D) and TUNEL positivity (E) in the ovary. (F-G) Comparison of ovarian tissue RNA expression between control, POI, and MSC mice. Relative gene expression level of the FSHR gene (F) and Cyp19 gene (G). (H) Morphology and marker protein expression in mouse endometrium (scale bar size: 300 μ m) (* $P < 0.05$, ** $P < 0.01$, *** $P < 0.001$). ER α : estrogen receptor α ; hBM-MSC: human bone marrow-derived mesenchymal stem cell; H&E: hematoxylin and eosin; POI: primary ovarian insufficiency; PR: progesterone receptor.

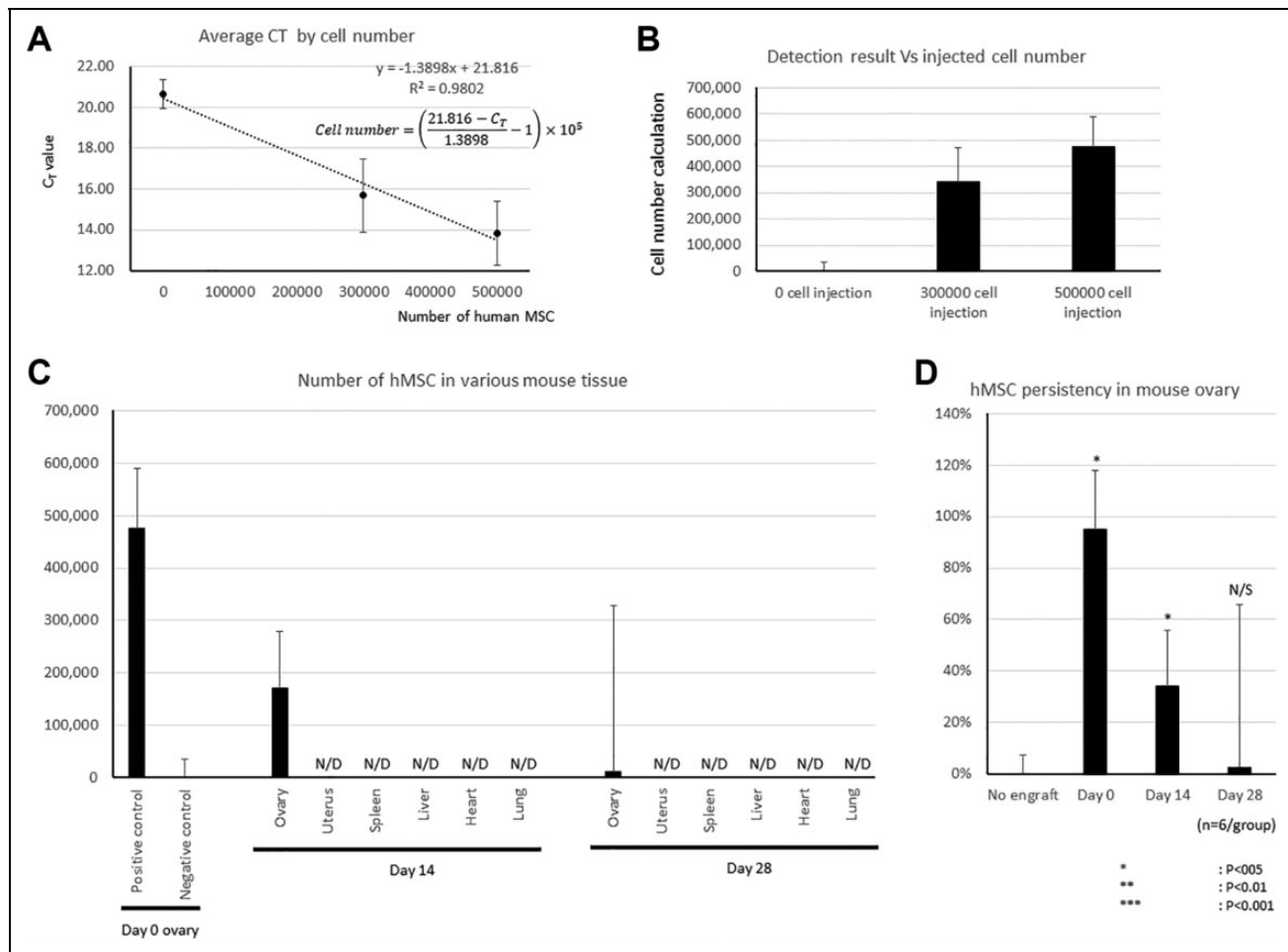


Figure 2. Polymerase chain reaction–based hBM-MSC detection in mouse tissue using ALU primers. (A) Correlation between CT value and the number of injected hBM-MSCs. (B) Calculation of the cell number quantification formula. (C) Quantification of the number of hBM-MSCs in various mouse tissues. (D) Persistency of injected hBM-MSCs in mouse ovary tissue. (* $P < 0.05$, ** $P < 0.01$, *** $P < 0.001$, N/D: not detected).

hBM-MSC: human bone marrow-derived mesenchymal stem cell.

another donor (Supplemental Figures 2, 3) and found similar results by PCR-based human cell detection. Our calculation of the persistence of engrafted hBM-MSCs in the ovary is shown in Fig. 2D. These results suggest that after intraovarian injection, engrafted hBM-MSCs do not migrate into other tissues, with more than 50% of the engrafted hBM-MSCs disappearing within 2 weeks after transplantation and most of the engrafted hBM-MSCs vanishing within 4 weeks after transplantation.

Human Stem Cell Distribution (by Ex Vivo Imaging) After Intraovarian Injection

To complement our PCR-based analysis and visualize engrafted cell distribution after injection, we next traced the distribution of injected hBM-MSCs through immunofluorescence imaging. We labeled hBM-MSCs with red fluorescing MIRB. Using fluorescence microscopy, we confirmed that more than 95% of cells were successfully labeled with MIRB (Fig. 3A). MIRB-labeled hBM-MSCs

were injected into the ovaries of two POI mice. One mouse was euthanized 24 h after injection, and the other mouse was euthanized on day 21 (14 days after pregnancy). Both mice were euthanized using CO₂ and frozen immediately in embedding media for ex vivo imaging. By 24 h after transplantation, most of the engrafted hBM-MSCs were located in the mouse ovary. Similar to our PCR-based analysis, at 21 days after transplantation, hBM-MSCs were present in the ovary, with no evidence of migration of labeled cells into other tissues or the embryo. These analyses demonstrated that engrafted hBM-MSCs by intraovarian injection remain in the target organ and do not migrate into other tissues.

Therapeutic Effect of Transplanted hBM-MSCs on Fertility in POI Mouse Model

Based on our PCR and imaging data, engrafted hBM-MSCs were not present in the POI mice beyond 28 days. To analyze

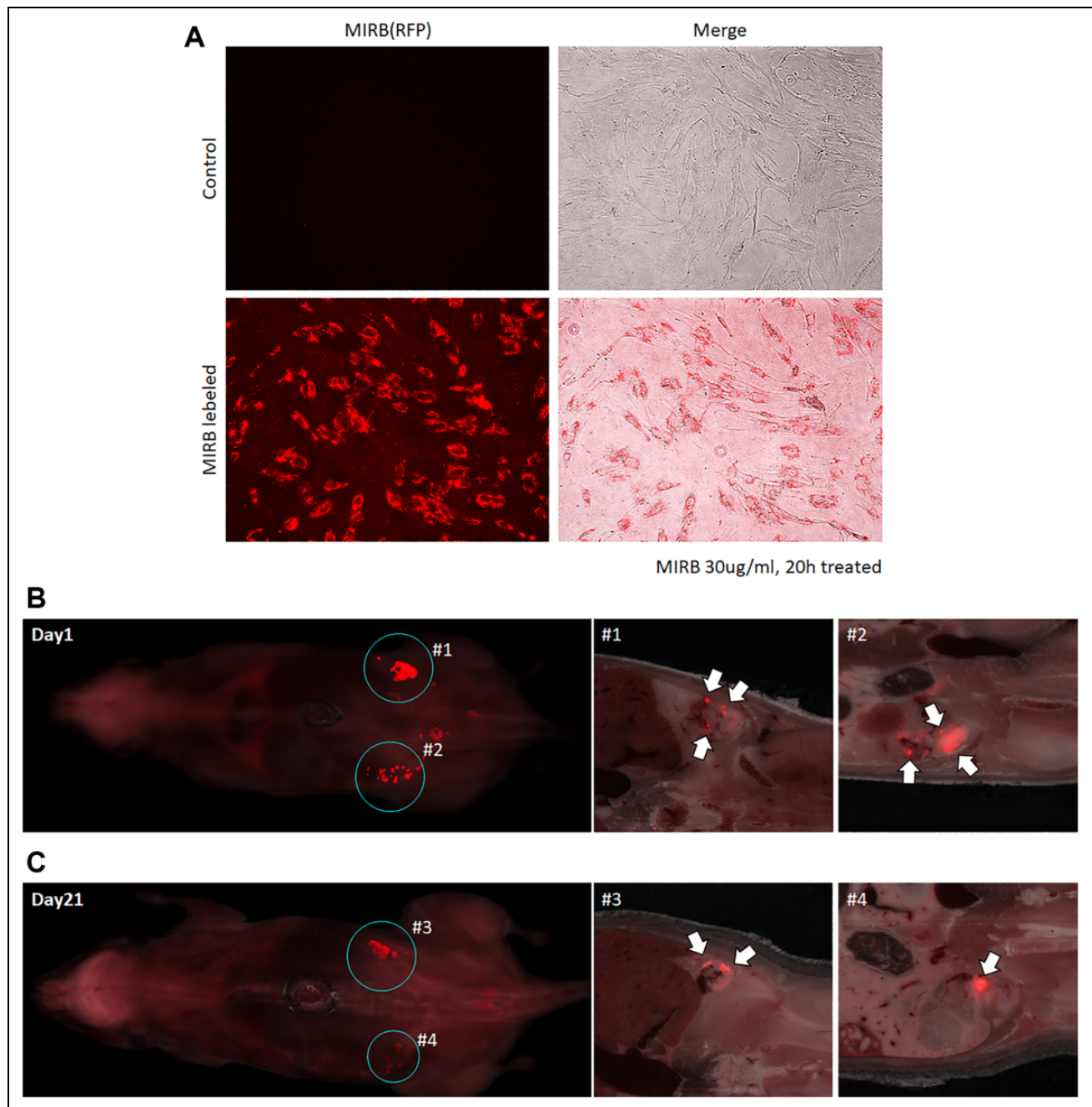


Figure 3. Detection of injected hBM-MSC by ex vivo imaging. (A) Fluorescence labeling of hBM-MSCs with MIRB. (B) Ex vivo imaging of the whole mouse body at day 1 after intraovarian injection. (C) Ex vivo imaging of the whole mouse body of a pregnant mouse on day 21 after intraovarian injection.

hBM-MSC: human bone marrow-derived mesenchymal stem cell; MIRB: Molday Iron Rhodamine B.

the effect of hBM-MSC transplantation on pregnancy, we performed a breeding experiment. One male mouse was housed with two female mice for 10 days. After the first litter delivery, mice were allowed to recover for 2 weeks, then the next round of breeding was resumed (Fig. 4A). We analyzed the pregnancy rate (number of pregnant mice/all mice) in each round of breeding and compared the

groups (Fig. 4B). In the first breeding round (7 to 42 days after hBM-MSC transplantation), the normal mouse group (control) showed an $83.3\% \pm 15.2\%$ pregnancy rate. The POI mouse group (POI) showed a significantly decreased pregnancy rate ($16.7\% \pm 15.2\%$). The hBM-MSC-treated POI mouse group (MSC) demonstrated a recovery in the pregnancy rate ($58.3\% \pm$

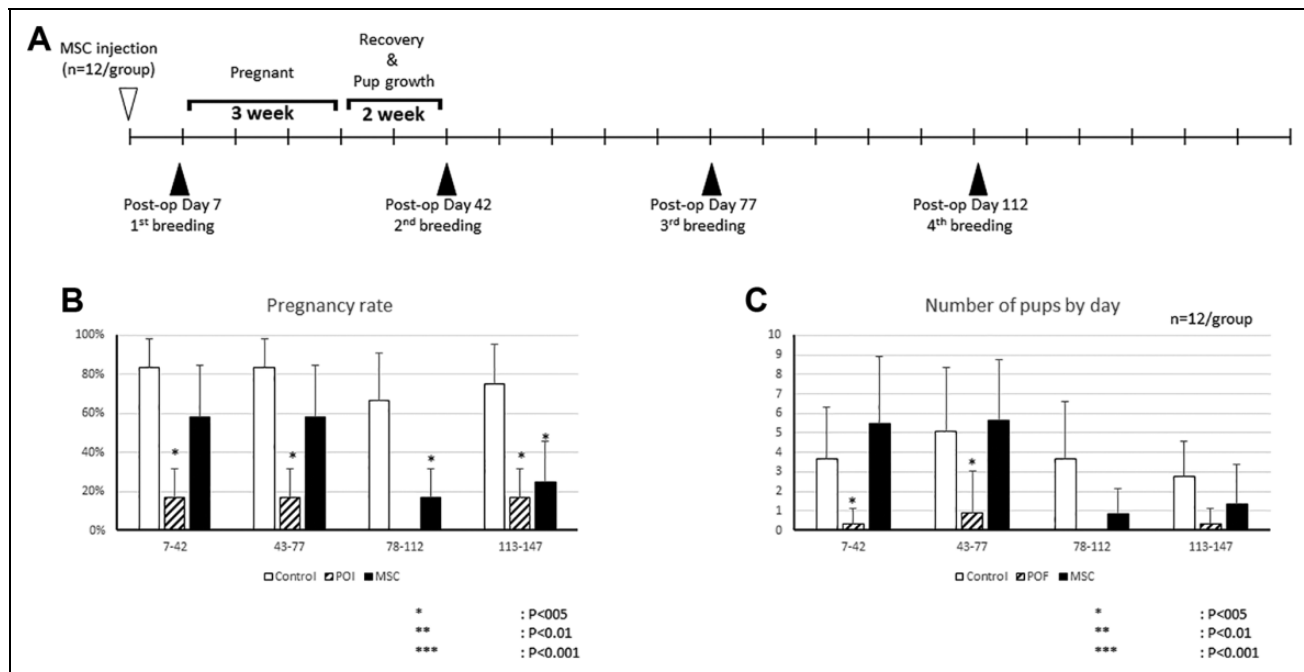


Figure 4. Restored fertility after hBM-MSC intraovarian injection. (A) Experimental plan for multiple breeding experiments. (B) Pregnancy rates in control, POI, and MSC mice in each breeding round. (C) Average number of pups in each breeding round (* $P < 0.05$, ** $P < 0.01$, *** $P < 0.001$).

hBM-MSC: human bone marrow-derived mesenchymal stem cell; POI: primary ovarian insufficiency.

26.5%), which was not significantly different compared to the control group. In the second round of breeding (43 to 77 days after hBM-MSC transplantation), the POI group again showed a lower pregnancy rate ($16.7\% \pm 15.2\%$) compared to controls, and the pregnancy rate was recovered in the MSC group ($58.3\% \pm 26.5\%$).

Interestingly, hBM-MSC transplantation did not restore the pregnancy rate in a third round of breeding (78 to 112 days after hBM-MSC transplantation). The pregnancy rate of the MSC group in the third breeding round was $16.7\% \pm 15.2\%$, significantly lower than that of the control group ($66.7\% \pm 24.2\%$). In a fourth breeding round (113 to 147 days after hBM-MSC transplantation), the control group mice showed a $75.0\% \pm 20.5\%$ of pregnancy rate; the rate was significantly lower in the POI group ($16.7\% \pm 15.2\%$) and MSC group ($25.0\% \pm 20.5\%$).

We also analyzed the average number of pups per mouse in each litter between the groups (Fig. 4C). In first litter, there were 3.67 ± 2.67 pups per mouse in the control group, 0.33 ± 0.78 pups per mouse in the POI group, and 5.50 ± 3.39 pups per mouse in the MSC group. The second litter showed a similar trend, with an average of 5.08 ± 3.28 pups in the control group, a decreased number of pups in the POI group (0.92 ± 2.15), and a restored number of pups in the MSC group (5.67 ± 3.08). Consistent with the pregnancy rate trends, the average number of pups in the third and fourth litters was not restored in the MSC group to the numbers seen in the control group. The average number of

pups in the third litter was 0.83 ± 1.33 and 1.33 ± 2.07 in the fourth litter in the MSC group. These results suggest that the effect of hBM-MSCs on the restoration of fertility diminishes after 78 days of cell transplantation.

Effect of hBM-MSC Engraftment on Offspring

Though we confirmed that engrafted hBM-MSCs do not stay in the host body beyond 4 weeks and no cells were detected in the embryo in our fluorescence imaging analysis, we evaluated the potential short-term effect of hBM-MSCs on offspring. We analyzed the presence of human DNA in mouse embryos and postnatal growth rate of pups from control mice and hBM-MSC-treated POI mice, which had been treated with hBM-MSCs from two different donors. We collected mouse embryos (7 to 10 days) and isolated genomic DNA for human-specific ALU PCR analysis (Fig. 5A-C). We did not detect any human DNA in the embryos from mice treated with hBM-MSCs from either donor.

The morphology and growth rate of pups was followed out to 10 days postnatal (Fig. 5D-F). No morphologic differences were seen in the pups from the control group and the hBM-MSC-treated group. All pups were visibly active in response and movement at postnatal day 0. At postnatal day 5, we observed hair growth in pups, and around day 10, all the pups were completely covered with black fur and were actively moving. The average body weight of control group

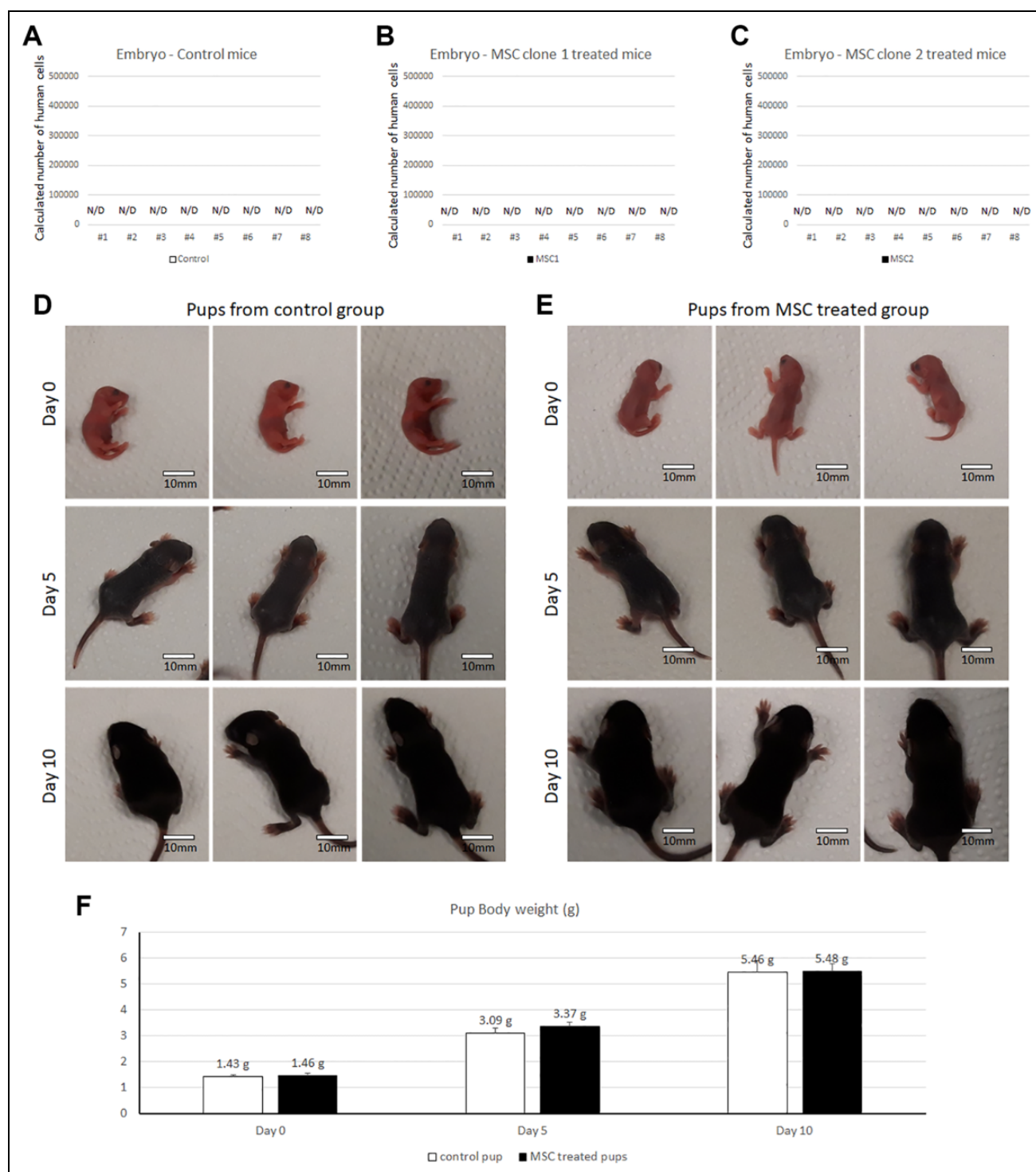


Figure 5. Effect of hBM-MSC intraovarian injection on offspring. (A-C) Detection of human cells in the embryo by PCR-based analysis using ALU primers. (D-E) Morphology of pups from a control mouse (D) and hBM-MSC-injected POI mouse (E) up to postnatal day 10. (F) Average body weight of mouse pups (scale bar size: 10 mm). hBM-MSC: human bone marrow-derived mesenchymal stem cell; POI: primary ovarian insufficiency.

pups and the hBM-MSC-treated group pups, respectively, was 1.45 ± 0.08 and 1.46 ± 0.10 g at day 0, 3.09 ± 0.20 g and 3.37 ± 0.17 g at day 5, and 5.46 ± 0.44 and 5.48 ± 0.32 g at day 10, without any significant difference

between the groups, signifying a normal growth rate. Taken together, intraovarian injection of hBM-MSCs did not result in human DNA integration into the offspring genome and had no effect on offspring postnatal growth.

Discussion

In this study, we provide preclinical evidence of the safety of intraovarian injection of hBM-MSCs in a mouse model of POI, using a well-established ALU PCR-based method for human cell detection²⁹. We also found that the engrafted hBM-MSCs did not migrate to any other major organs and almost disappeared from the host body by 4 weeks after transplantation. In addition, we found that the therapeutic effect of hBM-MSC transplantation on measures of fertility also diminished after 78 days of cell transplantation. Finally, we confirmed that transplanted hBM-MSCs do not affect the offspring postnatal growth rate.

The ultimate goal of our study is developing treatment using hBM-MSCs for restoring fertility in human patients with POI who are typically immune competent. Before applying our findings to human patients, the therapeutic effect and persistency of hBM-MSCs should be confirmed in as matched animal model as possible. Many studies used immune-compromised mice to enhance viability of engrafted cells in animal model. However, if we use immune-compromised POI mice model, it is hard to extrapolate the persistency of hBM-MSC transplantation in an actual immune-competent patient. To establish more realistic data for persistency of hBM-MSC, we used immune-competent POI mice model instead of immune-compromised model. Numerous reports suggested that human MSCs lack tissue surface antigens (major histocompatibility complex [MHC] I and MHC II)³⁰ as well as secrete immune-suppressive cytokines in their adjacent microenvironment such as interleukin 10 (IL-10) and TGFβ1 and as such elicit no or minimal host immune rejection^{15,31}.

Recent studies have suggested that MSCs may be a promising cell source for cell-based therapy. MSCs are easy to extract from various tissues³¹, and many previous studies have revealed that MSCs repair tissue via replacing injured cells by differentiation^{32–35}. In addition, MSCs can stimulate tissue regeneration by promoting angiogenesis and cell viability via paracrine activity through cytokines and extracellular vesicles^{15,36,37}. Various studies suggested interesting interaction between the paracrine effect of MSCs and the cell surrounding environment. In the published study, it was reported that the secreted factors highly depend on the external environment and the status of MSCs^{38,39}. Other studies also suggested different therapeutic mechanisms of MSC treatment through inflammatory regulation. Several studies revealed that some pro-inflammatory cytokines such as interleukin 6 and tumor necrosis factor alpha can induce MSC mitochondria transfer to rescue injured cells in various cell types^{40–42}. According to the published studies, it appears that a pro-inflammatory environment can enhance MSC mitochondria transfer to T cells to educate immune cells and this interaction eventually leads to restored inflammation and tissue damage⁴³. In this connection, MSC paracrine function and mitochondrial transfer capacity are interactive and linked together to promote the tissue regeneration.

For the therapeutic effect of MSCs on our POI model, our previous studies reported that intraovarian injection of MSCs restores fertility in a POI mouse model^{16,17}. Together, these published studies support allogeneic MSCs as a promising cell source to treat infertility in POI.

Recent studies suggest that MSCs are an ideal therapeutic cell source due to their dual tissue repair and immunosuppressive properties^{30,31}. In these studies, MSCs were shown to regulate immune cells by secreting various cytokines such as IL10, TGFβ, and VEGF³⁰. Despite these advantages, there are still several concerns about the use of allogeneic stem cells for transplantation, such as the risk of tumor formation. In this and our previous study, we analyzed the morphology of hBM-MSC-engrafted ovaries in multiple animals. H&E staining of the mouse ovary showed a normal appearance. Use of either an antibody for human cell-specific markers or fluorescence labeling of the injected cells has been well documented in the literature for tracking cells after injection^{17,44–46}. We found engrafted hBM-MSCs only in the injected tissue (ovary), with no migration of hBM-MSCs after 28 days. Moreover, the number of hBM-MSCs found in the ovary also decreased after transplantation, and more than 95% of engrafted cells had disappeared after 28 days of transplantation. Our findings are consistent with those of previous studies, which reported that mesenchymal stem cells do not produce teratoma or germ line-transmitting chimeras because they are not pluripotent stem cells^{47,48}. In addition, several papers reported that mesenchymal stem cells could inhibit tumor progression^{49,50}. These previous studies and our result suggest that hBM-MSCs are safe for stem cells, which are not forming tumor after transplantation.

Genomic integration is another major concern after allogeneic stem cell transplantation, especially when used as an infertility treatment. To address this safety issue, we analyzed human-specific sequences in various mouse tissues such as ovary, uterus, spleen, liver, heart, and lung, after hBM-MSC injection. Many studies suggest that PCR using ALU-specific primers can detect human genomic DNA in a small animal model with high sensitivity^{29,51–54}. Our ALU PCR analysis suggested that no human genes were incorporated into the host or embryos after hBM-MSC injection. Recent studies have reported that MSCs restore ovarian granulosa cells by secreting exosomes^{55–57}. Our previous study revealed that the effect of MSCs in the POI ovary involves a paracrine mechanism¹⁸. Based on our recent data and previously published studies, we conclude that engrafted hBM-MSCs in the POI ovary does not differentiate to replace ovarian cells, but instead restores ovarian granulosa cells by secreting paracrine stimulatory factors.

This study provides additional preclinical evidence that intraovarian injection of hBM-MSCs may be a promising and safe therapy for restoring ovarian function and fertility in POI patients. Today, the only option for POI patients to have a baby is through egg donation; however, this is not a solution for patients who want their own biological child.

The body of evidence continues to grow regarding the safety and efficacy of allogeneic MSCs, and clinical trials are now needed to test this approach as a new option to restore ovarian function in POI patients.

Conclusion

In our previous studies, we reported that intraovarian injection of hBM-MSCs restores fertility in a POI mouse model. However, the safety and effect of the transplanted cells on the recipient and offspring needed to be explored. In this study, we reported that the injected hBM-MSCs stay in the ovary and do not migrate to other tissues. The number of injected hBM-MSCs decreased by more than 50% within 2 weeks and disappeared entirely in most animals within 4 weeks after injection. In addition, while hBM-MSC treatment restored fertility, the effect diminished by 78 days following cell transplantation. Moreover, we revealed a lack of genetic integration from the injected cells in the offspring of treated mice, and that hBM-MSC treatment did not affect the postnatal growth of the offspring. Taken together, this study provides further evidence that intraovarian injection of hBM-MSCs may be a safe therapy for restoring fertility in POI, and clinical trials are needed to translate this option to treat female infertility in POI patients. Understanding the distribution of engrafted hBM-MSCs and the potential for human DNA transfer to offspring after hBM-MSC transplantation in an animal model will provide key preclinical safety data required for further clinical development and future applications of hBM-MSCs to the treatment of POI-associated infertility in women.

Author Contributions

Hang-soo Park and Rishi Man Chugh were equally involved in the experimental design, performed most experiments and data analysis, and wrote the manuscript. Hang-soo Park performed all *in vivo* experiments including surgery and tissue analysis. Rishi Man Chugh prepared hBM-MSC and participated in animal surgery. Amro Elsharoud, Mara Ulin, Sahar Esfandyari, Alshimaa Aboalsoud, and Lale Bakir helped with animal surgery, tissue collection, and PCR. Ayman Al-Hendy led the entire study as a corresponding author. All authors read and approved the final manuscript.

Ethical Approval

The experimental animal protocol in this study was approved by the University of Illinois at Chicago Animal Care Committee (UIC ACC/19-095).

Statement of Human and Animal Rights

All procedures in this study were performed in accordance with the ethical policy and guidelines of University of Illinois at Chicago for laboratory animals, and experimental protocol was approved by the University of Illinois at Chicago Animal Care Committee (UIC ACC/19-095).

Statement of Informed Consent

There are no human subjects in this article and informed consent is not applicable.


Declaration of Conflicting Interests

The author(s) declared no potential conflicts of interest with respect to the research, authorship, and/or publication of this article.

Funding

The author(s) disclosed receipt of the following financial support for the research, authorship, and/or publication of this article: This study was financially supported by a University of Chicago start-up funding to Ayman Al-Hendy.

ORCID iD

Hang-Soo Park  <https://orcid.org/0000-0002-9130-8478>

Supplemental Material

Supplemental material for this article is available online.

References

1. Beck-Peccoz P, Persani L. Premature ovarian failure. *Orphanet J Rare Dis.* 2006;1:9.
2. Christin-Maitre S, Braham R. General mechanisms of premature ovarian failure and clinical check-up [in French]. *Gynecol Obstet Fertil.* 2008;36(9):857–861.
3. Panay N, Fenton A. Premature ovarian failure: a growing concern. *Climacteric.* 2008;11(1):1–3.
4. Rebar RW. Premature ovarian failure. *Obstet Gynecol.* 2009; 113(6):1355–1363.
5. Shelling AN. Premature ovarian failure. *Reproduction.* 2010; 140(5):633–641.
6. Elfayomy AK, Almasry SM, El-Tarhouny SA, Eldomiaty MA. Human umbilical cord blood-mesenchymal stem cells transplantation renovates the ovarian surface epithelium in a rat model of premature ovarian failure: possible direct and indirect effects. *Tissue Cell.* 2016;48(4):370–382.
7. Blumenfeld Z, Evron A. Endocrine prevention of chemotherapy-induced ovarian failure. *Curr Opin Obstet Gynecol.* 2016;28(4):223–229.
8. Molina JR, Barton DL, Loprinzi CL. Chemotherapy-induced ovarian failure: manifestations and management. *Drug Saf.* 2005;28(5):401–416.
9. Blumenfeld Z. Chemotherapy and fertility. *Best Pract Res Clin Obstet Gynaecol.* 2012;26(3):379–390.
10. Lai D, Wang F, Dong Z, Zhang Q. Skin-derived mesenchymal stem cells help restore function to ovaries in a premature ovarian failure mouse model. *PLoS One.* 2014;9(5):e98749.
11. Morgan S, Anderson RA, Gourley C, Wallace WH, Spears N. How do chemotherapeutic agents damage the ovary?. *Hum Reprod Update.* 2012;18(5):525–535.
12. Chen L, Guo S, Wei C, Li H, Wang H, Xu Y. Effect of stem cell transplantation of premature ovarian failure in animal models and patients: a meta-analysis and case report. *Exp Ther Med.* 2018;15(5):4105–4118.

13. Fazeli Z, Abedindo A, Omrani MD, Ghaderian SMH. Mesenchymal stem cells (MSCs) therapy for recovery of fertility: a systematic review. *Stem Cell Rev Rep*. 2018;14(1):1–12.
14. Wang S, Yu L, Sun M, Mu S, Wang C, Wang D, Yao Y. The therapeutic potential of umbilical cord mesenchymal stem cells in mice premature ovarian failure. *Biomed Res Int*. 2013;2013:690491.
15. Fan XL, Zhang Y, Li X, Fu QL. Mechanisms underlying the protective effects of mesenchymal stem cell-based therapy. *Cell Mol Life Sci*. 2020;77(14):2771–2794.
16. Mohamed SA, Shalaby S, Brakta S, Elam L, Elsharoud A, Al-Hendy A. Umbilical cord blood mesenchymal stem cells as an infertility treatment for chemotherapy induced premature ovarian insufficiency. *Biomedicines*. 2019;7(1).
17. Mohamed SA, Shalaby SM, Abdelaziz M, Brakta S, Hill WD, Ismail N, Al-Hendy A. Human mesenchymal stem cells partially reverse infertility in chemotherapy-induced ovarian failure. *Reprod Sci*. 2018;25(1):51–63.
18. Park H-S, Ashour D, Elsharoud A, Chugh RM, Ismail N, Andaloussi AE, Al-Hendy A. Towards cell free therapy of premature ovarian insufficiency: human bone marrow mesenchymal stem cells secretome enhances angiogenesis in human ovarian microvascular endothelial cells. *J Stem Cells Res Dev Ther*. 2019;5(2):1–8.
19. Ben-David U, Benvenisty N. The tumorigenicity of human embryonic and induced pluripotent stem cells. *Nat Rev Cancer*. 2011;11(4):268–277.
20. Liang Y, Zhang H, Feng QS, Cai MB, Deng W, Qin D, Yun JP, Tsao GS, Kang T, Esteban MA, Pei D, et al. The propensity for tumorigenesis in human induced pluripotent stem cells is related with genomic instability. *Chin J Cancer*. 2013;32(4):205–512.
21. Ra JC, Shin IS, Kim SH, Kang SK, Kang BC, Lee HY, Kim YJ, Jo JY, Yoon EJ, Choi HJ, Kwon E. Safety of intravenous infusion of human adipose tissue-derived mesenchymal stem cells in animals and humans. *Stem Cells Dev*. 2011;20(8):1297–1308.
22. Wang Y, Han ZB, Song YP, Han ZC. Safety of mesenchymal stem cells for clinical application. *Stem Cells Int*. 2012;2012:652034.
23. Dlouhy BJ, Awe O, Rao RC, Kirby PA, Hitchon PW. Autograft-derived spinal cord mass following olfactory mucosal cell transplantation in a spinal cord injury patient: Case report. *J Neurosurg Spine*. 2014;21(4):618–622.
24. Lukomska B, Stanaszek L, Zuba-Surma E, Legosz P, Sarzynska S, Dreła K. Challenges and controversies in human mesenchymal stem cell therapy. *Stem Cells Int*. 2019;2019(2):9628536.
25. Liu T, Huang Y, Guo L, Cheng W, Zou G. CD44+/CD105+ human amniotic fluid mesenchymal stem cells survive and proliferate in the ovary long-term in a mouse model of chemotherapy-induced premature ovarian failure. *Int J Med Sci*. 2012;9(7):592–602.
26. Liu T, Huang Y, Zhang J, Qin W, Chi H, Chen J, Yu Z, Chen C. Transplantation of human menstrual blood stem cells to treat premature ovarian failure in mouse model. *Stem Cells Dev*. 2014;23(13):1548–1557.
27. McLean AC, Valenzuela N, Fai S, Bennett SA. Performing vaginal lavage, crystal violet staining, and vaginal cytological evaluation for mouse estrous cycle staging identification. *J Vis Exp*. 2012(67):e4389.
28. Cora MC, Kooistra L, Travlos G. Vaginal cytology of the laboratory rat and mouse: review and criteria for the staging of the estrous cycle using stained vaginal smears. *Toxicol Pathol*. 2015;43(6):776–793.
29. Funakoshi K, Bagheri M, Zhou M, Suzuki R, Abe H, Akashi H. Highly sensitive and specific Alu-based quantification of human cells among rodent cells. *Sci Rep*. 2017;7(1):13202.
30. Zhang J, Huang X, Wang H, Liu X, Zhang T, Wang Y, Hu D. The challenges and promises of allogeneic mesenchymal stem cells for use as a cell-based therapy. *Stem Cell Res Ther*. 2015;6:234.
31. Han Y, Li X, Zhang Y, Han Y, Chang F, Ding J. Mesenchymal stem cells for regenerative medicine. *Cells*. 2019;8(8):886.
32. Kim N, Cho SG. Clinical applications of mesenchymal stem cells. *Korean J Intern Med*. 2013;28(4):387–402.
33. Noth U, Osyczka AM, Tuli R, Hickok NJ, Danielson KG, Tuan RS. Multilineage mesenchymal differentiation potential of human trabecular bone-derived cells. *J Orthop Res*. 2002;20(5):1060–1069.
34. Pittenger MF, Mackay AM, Beck SC, Jaiswal RK, Douglas R, Mosca JD, Moorman MA, Simonetti DW, Craig S, Marshak DR. Multilineage potential of adult human mesenchymal stem cells. *Science*. 1999;284(5411):143–147.
35. Satue M, Schuler C, Ginner N, Erben RG. Intra-articularly injected mesenchymal stem cells promote cartilage regeneration, but do not permanently engraft in distant organs. *Sci Rep*. 2019;9(1):10153.
36. Caplan AI, Dennis JE. Mesenchymal stem cells as trophic mediators. *J Cell Biochem*. 2006;98(5):1076–1084.
37. Fan XL, Zhang Z, Ma CY, Fu QL. Mesenchymal stem cells for inflammatory airway disorders: promises and challenges. *Biosci Rep*. 2019;39(1):BSR20182160.
38. Siu CW, Liao SY, Liu Y, Lian Q, Tse HF. Stem cells for myocardial repair. *Thromb Haemost*. 2010;104(1):6–12.
39. Zhang Y, Liang X, Lian Q, Tse HF. Perspective and challenges of mesenchymal stem cells for cardiovascular regeneration. *Expert Rev Cardiovasc Ther*. 2013;11(4):505–517.
40. Jiang D, Xiong G, Feng H, Zhang Z, Chen P, Yan B, Chen L, Gandhervin K, Ma C, Li C, Han S, et al. Donation of mitochondria by iPSC-derived mesenchymal stem cells protects retinal ganglion cells against mitochondrial complex I defect-induced degeneration. *Theranostics*. 2019;9(8):2395–2410.
41. Yao Y, Fan XL, Jiang D, Zhang Y, Li X, Xu ZB, Fang SB, Chiu S, Tse HF, Lian Q, Fu QL. Connexin 43-mediated mitochondrial transfer of iPSC-MSCs alleviates asthma inflammation. *Stem Cell Reports*. 2018;11(5):1120–1135.
42. Zhang Y, Yu Z, Jiang D, Liang X, Liao S, Zhang Z, Yue W, Li X, Chiu SM, Chai YH, Liang Y, et al. iPSC-MSCs with high intrinsic MIRO1 and sensitivity to TNF-alpha yield efficacious mitochondrial transfer to rescue anthracycline-induced cardiomyopathy. *Stem Cell Reports*. 2016;7(4):749–763.

43. Court AC, Le-Gatt A, Luz-Crawford P, Parra E, Aliaga-Tobar V, Batiz LF, Contreras RA, Ortuzar MI, Kurte M, Elizondo-Vega R, Maracaja-Coutinho V, et al. Mitochondrial transfer from MSCs to T cells induces Treg differentiation and restricts inflammatory response. *EMBO Rep.* 2020;21(2):e48052.
44. Alawadhi F, Du H, Cakmak H, Taylor HS. Bone marrow-derived stem cell (BMDSC) transplantation improves fertility in a murine model of Asherman's syndrome. *Plos One.* 2014;9(5):e96662.
45. Mas A, Nair S, Laknaur A, Simon C, Diamond MP, Al-Hendy A. Stro-1/CD44 as putative human myometrial and fibroid stem cell markers. *Fertil Steril.* 2015;104(1):225–234 e3.
46. Nicholls FJ, Liu JR, Modo M. A comparison of exogenous labels for the histological identification of transplanted neural stem cells. *Cell Transplant.* 2017;26(4):625–645.
47. Gruenloh W, Kambal A, Sondergaard C, McGee J, Nacey C, Kalomoiris S, Pepper K, Olson S, Fierro F, Nolte JA. Characterization and *in vivo* testing of mesenchymal stem cells derived from human embryonic stem cells. *Tissue Eng Part A.* 2011;17(11-12):1517–1525.
48. Wakao S, Kuroda Y, Ogura F, Shigemoto T, Dezawa M. Regenerative effects of mesenchymal stem cells: contribution of muse cells, a novel pluripotent stem cell type that resides in mesenchymal cells. *Cells.* 2012;1(4):1045–1060.
49. He N, Kong Y, Lei X, Liu Y, Wang J, Xu C, Wang Y, Du L, Ji K, Wang Q, Li Z, et al. MSCs inhibit tumor progression and enhance radiosensitivity of breast cancer cells by down-regulating Stat3 signaling pathway. *Cell Death Dis.* 2018;9(10):1026.
50. Lin W, Huang L, Li Y, Fang B, Li G, Chen L, Xu L. Mesenchymal stem cells and cancer: clinical challenges and opportunities. *Biomed Res Int.* 2019;2019:2820853.
51. McBride C, Gaupp D, Phinney DG. Quantifying levels of transplanted murine and human mesenchymal stem cells *in vivo* by real-time PCR. *Cytherapy.* 2003;5(1):7–18.
52. Nicklas JA, Buel E. Simultaneous determination of total human and male DNA using a duplex real-time PCR assay. *J Forensic Sci.* 2006;51(5):1005–1015.
53. Preston Campbell J, Mulcrone P, Masood SK, Karolak M, Merkel A, Hebron K, Zijlstra A, Sterling J, Elefteriou F. -TRIZol and Alu qPCR-based quantification of metastatic seeding within the skeleton. *Sci Rep.* 2015;5:12635.
54. Zhang W, Wu M, Menesale E, Lu T, Magliola A, Bergelson S. Development and qualification of a high sensitivity, high throughput Q-PCR assay for quantitation of residual host cell DNA in purification process intermediate and drug substance samples. *J Pharm Biomed Anal.* 2014;100:145–149.
55. Liu M, Qiu Y, Xue Z, Wu R, Li J, Niu X, Yuan J, Wang Y, Wu Q. Small extracellular vesicles derived from embryonic stem cells restore ovarian function of premature ovarian failure through PI3K/AKT signaling pathway. *Stem Cell Res Ther.* 2020; 11(1):3.
56. Sun L, Li D, Song K, Wei J, Yao S, Li Z, Su X, Ju X, Chao L, Deng X, Kong B, et al. Exosomes derived from human umbilical cord mesenchymal stem cells protect against cisplatin-induced ovarian granulosa cell stress and apoptosis *in vitro*. *Sci Rep.* 2017;7(1):2552.
57. Yang M, Lin L, Sha C, Li T, Zhao D, Wei H, Chen Q, Liu Y, Chen X, Xu W, Li Y, et al. Bone marrow mesenchymal stem cell-derived exosomal miR-144-5p improves rat ovarian function after chemotherapy-induced ovarian failure by targeting PTEN. *Lab Invest.* 2020;100(3):342–352.